Am J Physiol Gastrointest Liver Physiol 311: G40–G49, 2016.
First published May 5, 2016; doi:10.1152/ajpgi.00435.2015.

Mechanisms of innate immune activation by gluten peptide p31-43 in mice

Romina E. Araya,[1] María Florencia Gomez Castro,[1] Paula Carasi,[2] Justin L. McCarville,[3] Jennifer Jury,[3] Allan M. Mowat,[4] Elena F. Verdu,[3] and Fernando G. Chirdo[1]

[1]*Instituto de Estudios Inmunológicos y Fisiopatológicos (IIFP)(CONICET-UNLP), Facultad de Ciencias Exactas, Universidad Nacional de La Plata, La Plata, Argentina;* [2]*Catedra de Microbiología, Facultad de Ciencias Exactas, Universidad Nacional de La Plata, La Plata, Argentina;* [3]*Farncombe Family Digestive Health Research Institute, McMaster University, Hamilton, Ontario, Canada;* [4]*Centre for Immunobiology, Institute of Infection, Immunity and Inflammation, University of Glasgow, Glasgow, Scotland, United Kingdom*

Submitted 9 December 2015; accepted in final form 2 May 2016

Araya RE, Gomez Castro MF, Carasi P, McCarville JL, Jury J, Mowat AM, Verdu EF, Chirdo FG. Mechanisms of innate immune activation by gluten peptide p31-43 in mice. *Am J Physiol Gastrointest Liver Physiol* 311: G40–G49, 2016. First published May 5, 2016; doi:10.1152/ajpgi.00435.2015.—Celiac disease (CD) is an immune-mediated enteropathy triggered by gluten in genetically susceptible individuals. Innate immunity contributes to the pathogenesis of CD, but the mechanisms remain poorly understood. Although previous in vitro work suggests that gliadin peptide p31-43 acts as an innate immune trigger, the underlying pathways are unclear and have not been explored in vivo. Here we show that intraluminal delivery of p31-43 induces morphological changes in the small intestinal mucosa of normal mice consistent with those seen in CD, including increased cell death and expression of inflammatory mediators. The effects of p31-43 were dependent on MyD88 and type I IFNs, but not Toll-like receptor 4 (TLR4), and were enhanced by coadministration of the TLR3 agonist polyinosinic:polycytidylic acid. Together, these results indicate that gliadin peptide p31-43 activates the innate immune pathways in vivo, such as IFN-dependent inflammation, relevant to CD. Our findings also suggest a common mechanism for the potential interaction between dietary gluten and viral infections in the pathogenesis of CD.

celiac disease; innate immunity; p31-43; polyinosinic:polycytidylic acid; small intestine

CELIAC DISEASE (CD) is a multifactorial disorder triggered by the ingestion of gluten in susceptible individuals who carry the HLA-DQ2 and/or HLA-DQ8 predisposing alleles. Both innate and adaptive immune mechanisms are involved in the pathogenesis of CD. Whereas the adaptive immune response has been well studied, less is known about innate mechanisms and their triggers (1). Some gluten-derived peptides could initiate this process, but there is not enough in vivo experimental evidence to confirm this hypothesis. The study of whether and how innate immune mechanisms are induced by gluten peptides is relevant to CD pathophysiology.

Several nonimmunogenic gluten peptides that stimulate innate immune responses (termed toxic peptides) but not the adaptive immune response have been proposed. Studies have shown that a mix of gluten peptides or pepsin-trypsin-digested gliadin (PT-gliadin) can activate dendritic cells (26) and peripheral blood mononuclear cells (16) in vitro. However, the peptides responsible have not been identified. The most studied toxic peptide is the derived α-gliadin p31-43 (LGQQQPFPPQQPY) that is part of the longer peptide p31-55 (LGQQQPFPPQQPYPQPQPFPSQQPY) and is resistant to digestive enzymes in the gut (19). Increased IL-15 production and enterocyte apoptosis were reported in duodenal biopsies of patients with CD incubated with p31-43 (18). p31-43 was also shown to interact with epidermal growth factor receptor (EGFR) (5) and with the IL-15/IL-15R complex (6, 24) to affect proliferative activity in intestinal biopsies, influence human fibroblasts (23), and induce oxidative stress and endosome maturation in enterocytes (17). In murine tissues, p31-43 induced proinflammatory cytokines by macrophages (34). Altogether, these studies suggest a role for p31-43 in the stimulation of innate immune mechanisms in CD. However, the underlying pathways and in vivo relevance remain unclear.

Type I IFNs are thought to play a role in CD pathogenesis, as there is increased expression of IFN-α in duodenal mucosa from patients with CD (22) and blockade of IFN-α inhibits gliadin-induced IFN-γ expression in ex vivo experiments (28). Furthermore, epidemiological studies suggest that enteric viral infections such as rotavirus might trigger inflammatory or functional gastrointestinal disease (20, 35). The aim of this study was to determine whether p31-43 elicits innate immune activation in murine small intestine in vivo and to investigate potential underlying pathways. We also analyzed the effect of combined intraluminal administration of p31-43 and polyinosinic:polycytidylic acid (poly I:C), which mimics a viral infection, a proposed trigger of CD.

MATERIALS AND METHODS

Mice. Eight-week-old male C57BL/6J mice were purchased from the Animal Care Facility of the Facultad de Ciencias Exactas y Naturales of the Universidad de Buenos Aires. Eight-week-old male MyD88 KO [B6.129P2(SJL)-Myd88tm1.1Defr/J] mice were purchased from the Jackson Laboratory. IFNαR knockout (KO) mice (IFNαβR$^{-/-}$, IFNαR$^{-/-}$) on C57BL/6 background were kindly provided by M. Albert (Institute Pasteur, Paris, France). Eight-week-old male C3H-HeJ mice were kindly provided by Dr. Martin Rumbo from Instituto de Estudios Inmunológicos y Fisiopatológicos (IIFP-CONICET, Buenos Aires, Argentina). Mice were housed in a specific pathogen-free condition and fed ad libitum with balanced food and autoclaved water. They were maintained on a 12-h:12-h light/dark cycle and acclimatized to the surrounding conditions for 1 wk before the experimental procedures. All the studies were performed in accordance with international protocols for laboratory animal care (Canadian Council on Animal Care). Experiments were conducted with approval from the Institutional Animal Care and Use Committee of the Facultad de Ciencias Exactas, Universidad Nacional de La Plata.

Address for reprint requests and other correspondence: F. Chirdo, Instituto de Estudios Inmunológicos y Fisiopatológicos (IIFP)(CONICET-UNLP), Facultad de Ciencias Exactas, Universidad Nacional de La Plata, La Plata, Argentina (e-mail: fchirdo@gmail.com)

Intraluminal administration of peptides and poly I:C. p31-43 peptide (LGQQQPFPPQQPY, Biomatik), nonrelated peptide (NRP) (LDPLIRGLLARPACALQV, Think Peptides), poly I:C (Sigma Aldrich), a combination of p31-43 peptide and poly I:C, or PBS were administered intraluminally during intestinal microsurgery as previously described (3). Briefly, mice were anaesthetized with 80 mg/kg ketamine and 10 mg/kg xylazine. Once asleep, 100 μl of 100 μg/ml peptide solution in PBS, 30 μg/g poly I:C solution, or a combination of p31-43 and poly I:C were injected into the small intestinal lumen, 2 cm below the pylorus, to avoid degradation by pancreatic enzymes. Control mice received PBS. After surgery, fluid replacement was administered, and mice were monitored until recovery. C57BL/6 mice were killed 2–72 h posttreatment, whereas C3H-HeJ, IFNαR KO, and MyD88 KO mice were killed 12 h posttreatment.

To compare the effects of p31-43, poly I:C, and p31-43 + poly I:C in C57BL/6 mice, histological evaluation was performed at 72 h posttreatment. This time point was chosen based on the previous finding indicating significant differences between treatments at this time.

Histological evaluation. Sections of proximal small intestine of treated mice were fixed in 10% formalin, embedded in paraffin, and stained with hematoxylin and eosin for histological evaluation using a Nikon Eclipse Ti fluorescence microscope with X-Cites Series 120 Q light source. Images were taken with Nikon Digital Sight DS Ri1 camera using Nis-Elements software, and measurements were performed using Image J software.

Two sections of the proximal small intestine were scored for inflammation in a blinded fashion, with at least 30 villus-to-crypt (V/C) ratios assessed in each mouse. Intraepithelial lymphocytes (IELs) per 30 enterocytes in 10 randomly chosen villus tips were counted according to previously described methods and expressed as IELs/100 enterocytes (7). Histological scores were obtained following the Park-Chiu criteria (27): 0, normal mucosa; 1, subepithelial space at villus tips; 2, extension of subepithelial space with moderate lifting; 3, massive lifting down sides of villi, some denuded tips; 4, denuded villi, dilated capillaries; 5, disintegration of lamina propria; 6, crypt layer injury; 7, transmucosal infarction; 8, transmural infarction.

Real-time PCR. Small intestinal samples from C57BL/6 mice were stored in RNALater at −80°C until use. Tissues were disrupted, and RNA extraction was performed using RNeasy Mini Kit (Qiagen). cDNA synthesis was performed from isolated RNA samples (2–5 μg), using iScript Reverse Transcription Supermix (Bio-Rad). Real-time PCR was performed with SsoFastEvaGreen Supermix (Bio-Rad) using appropriate forward and reverse primers and the iQ5 thermocycler with fluorescence detection (Bio-Rad). Reactions were run in triplicate. The real-time PCR (qPCR) protocol was as follows: cycle 1 (1×) 95°C for 10 min; cycle 2 (40×) 60°C for 1 min and 95° for 15 s. Primers were synthesized as described previously (9) (Table 1). The geometric mean of housekeeping gene *HPRT* was used as an internal control to normalize the variability in expression levels. All results were expressed as fold increase of each treatment vs. the mean of PBS treatment in every time point ($2^{-\Delta\Delta Ct}$ method).

Isolation of epithelial cells and flow cytometric analysis. Sections of proximal small intestine (10 cm) of PBS- and p31-43-treated C57BL/6 mice were collected into cold calcium and magnesium-free HBSS (Gibco). Tissue sections were then incubated in HBSS containing 2% vol/vol FBS (Gibco) and 0.1 mM DTT (Sigma) at 4°C for 10 min before being incubated for 15 min at 37°C in HBSS with 0.5 mM EDTA (Sigma) with shaking. The cell suspensions were then filtered through an 80-μm filter mesh (BD Biosciences) before use. One million cells were used for flow cytometry analysis, and the remaining cells were stored in RNALater (Ambion) for real-time PCR analysis of Bax and Bcl2 mRNA expression as described above. For flow cytometric analysis, cells were washed twice with annexin V binding buffer and incubated for 30 min at room temperature using annexin V-FITC (Immunotools). One minute before cell acquisition propidium iodide (5 μg/tube) was added. Cells were analyzed in a BD FACSCalibur flow cytometer (BD Bioscience), and data were processed using CELLQest (BD Bioscience) software.

Table 1. *Primers used for quantitative PCR*

Gene	Forward	Reverse
HPRT	CAATGCAAACTTTGCTTTCC	CAAATCCAACAAAGTCTGGC
IFNβ	AATGGAAAGATCAACCTCAC	AAGGCAGTGTAACTCTTCTG
CXCL10	ATAGGGAAGCTTGAAATCATCC	TTCATCGTGGCAATGATCTC
CXCR3	TGTAGTTGGGCTAGCTCGAACTT	ACCTGGATATATGCTGAGCTGTCA
TNFα	CTCCCTCTCATCAGTTCTATGG	TTGAGAAGATGATCTGAGTGTG
IL-15	CATCCATCTCGTGCTACTTGTGTT	CATCTATCCAGTTGGCCTCTGTTT
MCP1	CTACAAGAGGATCACCAGCAG	TTCTGATCTCATTTGGTTCCG
CXCL2	AAGATACTGAACAAAGGCAAGG	TTCTTTCTCTTTGGTTCTTCCG
IL-1β	CGTTCCCATTAGACAACTGC	CTCATGGAGAATATCACTTGTTGG
IL-18	GATCAAAGTGCCAGTGAACC	GATCTTGTTCTTACAGGAGAGG
IL-6	CATGTTCTCTGGGAAATCGT	TATATCCAGTTTGGTAGCATCC
IFNγ	CTGAGACAATGAACGCTACAC	TTTCTTCCACATCTATGCCAC
Bax	TGCTACAGGGTTTCATCCAG	ATTGCTGTCCAGTTCATCTC
BclII	GATCTCTGGTTGGGATTCCT	ACAACTTGCAATGAATCGGG

Confocal microscopy. Small intestinal sections were deparaffinized and treated with Antigen Retrieval AR-10 Solution (BioGenex). After the sections were blocked with 2% goat serum, a primary antibody was added for 1 h. Anti-Ki-67 antibody (Novus Biologicals) was added at 4°C, and Alexa488 goat anti-rabbit antibody (Molecular Probes) was added at 10 μg/ml for 1 h. Anti-cleaved caspase-3 antibody conjugated to FITC (Cell Signaling) was added for 1 h at RT. Nuclei were stained with propidium iodide at 1 μg/ml for 15 min. Images were obtained and analyzed in a TCS SP5 Confocal Microscope combined with Leica LAS AF software.

TUNEL reaction. Cell death was quantified using the In Situ Cell Death Detection Kit (Roche). Paraffin-embedded small intestinal tissue sections were dewaxed, rehydrated, and treated with Proteinase K for permeabilization. TUNEL reaction mixture was then added, and samples were analyzed by confocal microscopy. Images were taken from a confocal microscope Olympus FV1000 using a ×20 NA 0.75 objective and a zoom of ×2. A 473-nm solid-state laser was used to detect apoptotic cells, whereas a 405-nm state laser was used to identify nuclei stained with DAPI. Images were analyzed with ImageJ software.

Statistical analysis. Statistical analysis was performed with GraphPad Prism software. When two groups were compared, an unpaired *t*-test was used. When more than two groups were compared, a one-way ANOVA test was used; $P < 0.05$ was considered significant. Data are displayed as means ± SE.

RESULTS

Intraluminal p31-43 peptide induces pathological changes in the murine small intestine. We used a previously developed technique to deliver molecules of interest intraluminally (3) and tested the capacity of p31-43 to induce morphological changes in small intestinal mucosa. At 12 h post p31-43 administration, we observed shortening and widening of villi, increased cell infiltration in the lamina propria, and edema. Administration of PBS or NRP did not cause intestinal damage (Fig. 1*A*). At this time point, we also observed reduction in V/C ratios, increased IEL counts, and higher histological scores in mice treated with p31-43 compared with PBS and NRP (Fig. 1*B*). At 72 h, mice treated with p31-43 exhibited persistent edema and cellular infiltration in the lamina propria (Fig. 1*A*), reduced V/C ratios, increased number of IELs, and a higher histological score compared with PBS- and NRP-treated mice (Fig. 1*B*). Although the surgical procedure itself altered intestinal histology transiently (3), PBS- and NRP-treated mice (controls) experienced faster recovery than p31-43-treated mice (Fig. 1*B*). We also evaluated the proliferative activity in

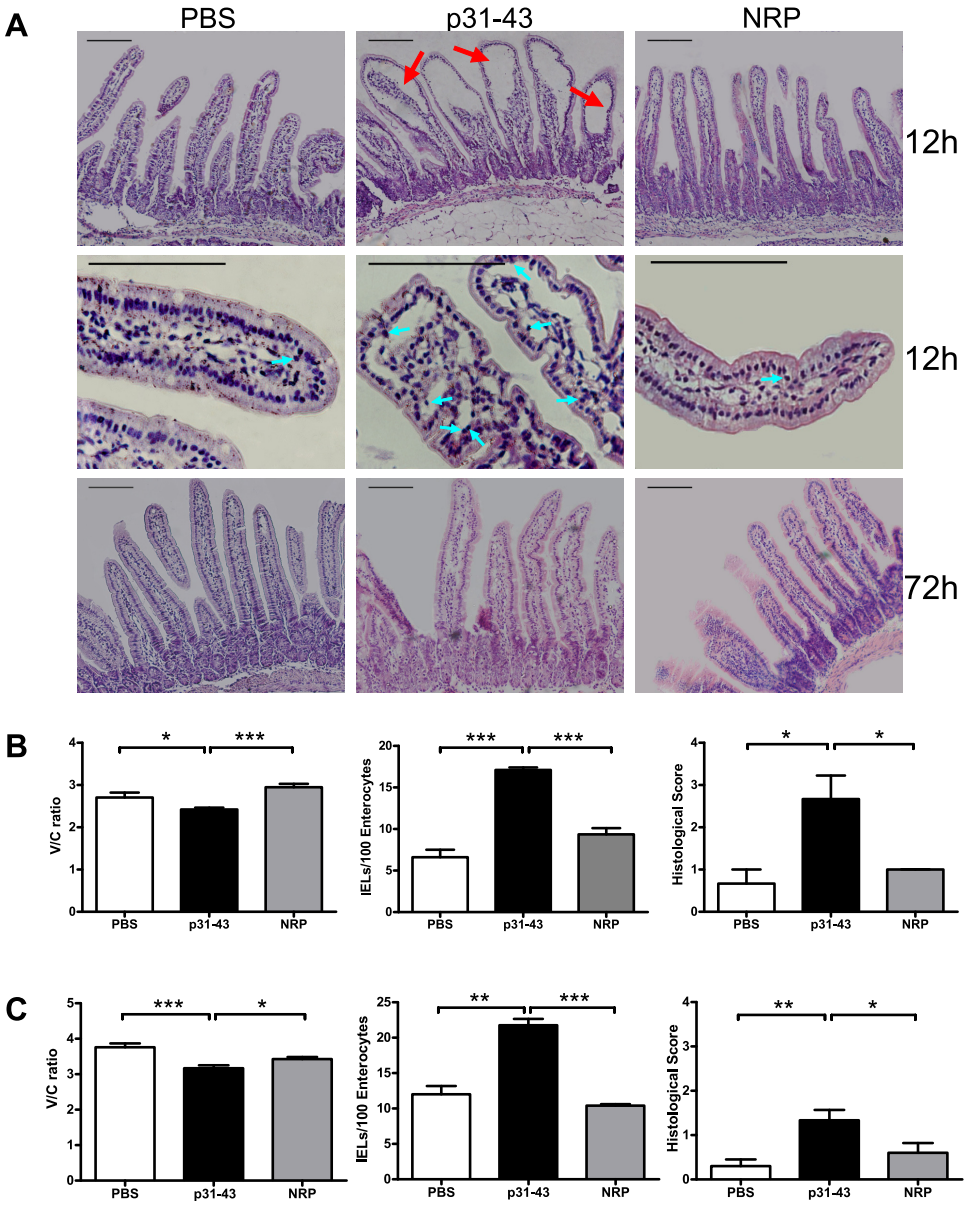

Fig. 1. Intraluminal p31-43 peptide induces pathological changes in the murine small intestine. Representative hematoxylin and eosin (H and E)-stained sections of proximal small intestine of C57BL/6 mice after 12 and 72 h of intraluminal administration of p31-43, nonrelated peptide (NRP), or PBS. Black scale bar = 100 μm. Red arrows show edema, and light blue arrows show some intraepithelial lymphocytes (IELs) (*A*). Morphological analysis of small intestine from C57BL/6 mice includes villus-to-crypt (V/C) ratio, number of IELs, and histological score after 12 h (*B*) and 72 h (*C*) ($n = 4$ mice per group, unpaired *t*-test, $^{*}P < 0.05$, $^{**}P < 0.01$, $^{***}P < 0.001$).

small intestinal crypts by counting Ki-67^{+} epithelial cells. At 12 h, proliferative activity was significantly higher in p31-43- than in PBS-treated mice (Fig. 2*A*).

Intraluminal p31-43 increases mRNA expression of inflammatory cytokines. We next explored the expression of proinflammatory mediators induced by p31-43. Compared with PBS-treated mice, there was a rapid and marked increase in IFN-γ mRNA 2 h after p31-43 treatment, followed by increases in CXCL10 and IFN-β mRNA, which peaked 6 h after intraluminal administration of p31-43 (Fig. 2*B*). The expression of mRNA for IL-15, IL-18, IL-1β, IL-6, TNF-α, and chemokines such as MCP1, CXCR3, and CXCL2 was similar in all groups (data not shown).

Intraluminal p31-43 induces cell death in the mucosa. Cell death by gluten-specific and -nonspecific cytotoxic mechanisms plays a role in intestinal damage in CD (31). To study whether p31-43 has cytotoxic activity, we examined TUNEL staining of small intestinal sections 12 h after treatment. This revealed a large increase in the number of TUNEL-positive cells in the lamina propria compared with PBS-treated mice (Fig. 3*A*). TUNEL-positive cells were also found in the epithelium of p31-43-treated but not in PBS-treated mice (white arrows, Fig. 3*A*). Automated counting confirmed an increase in the frequency of total TUNEL-positive cells, when both the lamina propria and epithelium of p31-43-treated mice were analyzed (Fig. 3*B*). The expression of anti- and proapoptotic mediators, Bcl2 and Bax, respectively, was evaluated by qPCR analysis of whole small intestinal mucosa. At 12 h, we found increased Bax/Bcl2 ratio in p31-43-treated mice compared with PBS-treated controls (Fig. 3*C*), suggesting that p31-43 has a proapoptotic effect in the small intestine in vivo. Mice treated with p31-43 had increased numbers of TUNEL-positive cells in epithelium compared with PBS-treated control mice (Fig. 3*D*). A similar trend was seen in lamina propria alone although this did not attain statistical significance. To further explore the hypothesis that p31-43 caused death of epithelial cells, we first

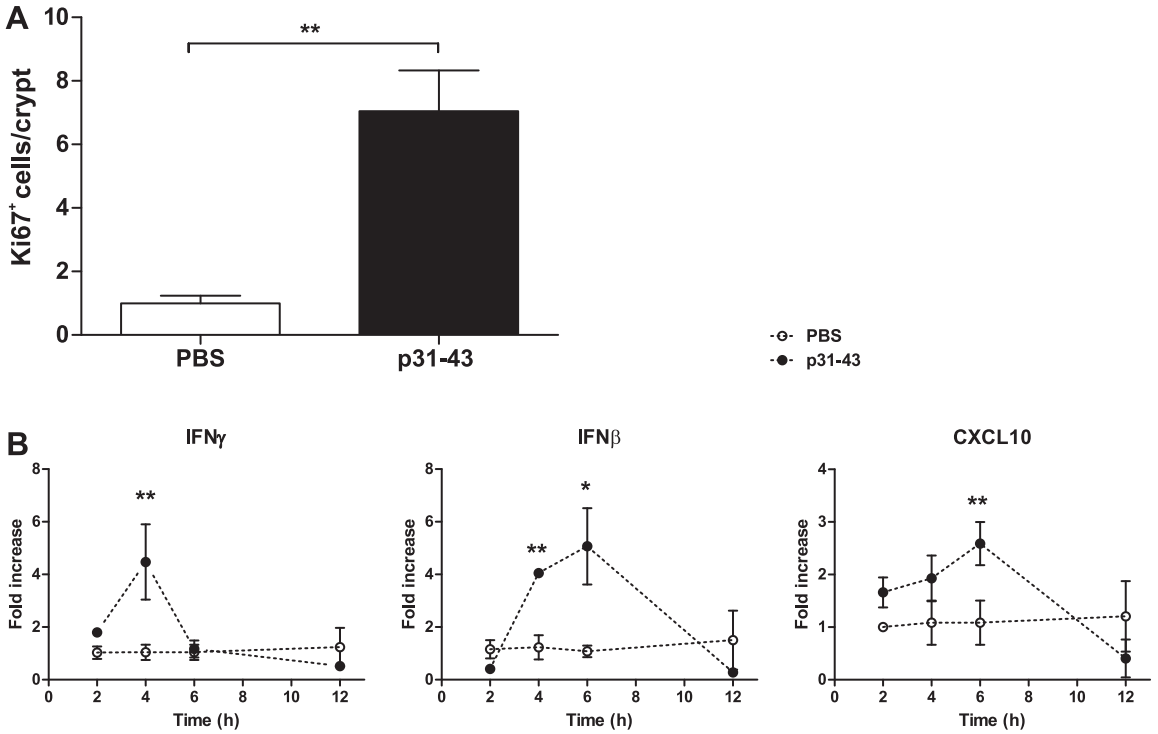

Fig. 2. Intraluminal p31-43 peptide produces hyperproliferation in crypts and a proinflammatory response in small intestine. Evaluation of the proliferative activity in small intestinal crypts by Ki-67-positive cell counts is shown. After 12 h posttreatment with p31-43 or PBS, samples of small intestine were stained with anti-Ki67 antibody. Images were obtained and analyzed in a TCS SP5 confocal microscope. The plots show the number of Ki-67-positive cells per crypt ($n = 4$ mice per group, unpaired t-test, $^{**}P < 0.01$) (*A*). Real-time PCR analysis of small intestinal samples from C57BL/6 mice after intraluminal administration of p31-43 or PBS was performed. Plots show mRNA expression after 2–12 h of p31-43 (●) or PBS (○) treatment. IFN-γ, IFN-β, and CXCL10 mRNA expression was assessed. All values were normalized with the housekeeping mRNA expression (HPRT). Results were expressed as fold increase of every treatment vs. the mean of PBS treatment in every time point ($2^{-\Delta\Delta Ct}$ method) ($n = 4$ mice per group, unpaired t-test, $^{*}P < 0.05$, $^{**}P < 0.01$, p31-43-treated mice vs. PBS control in the same time point).

used qPCR analysis of isolated epithelial cells, which showed a trend toward an increase in the Bax/Bcl2 ratio in intraepithelial cells (IEC) from p31-43-treated mice. Although this difference did not reach statistical significance (Fig. 3*E*), flow cytometry showed an increased number of annexin V-positive/propidium iodide-positive IECs from mice treated with p31-43 (Fig. 3*F*).

Mucosal changes induced by p31-43 are MyD88 and type I IFN dependent but not Toll-like receptor 4 dependent. To investigate possible signaling pathways that might mediate the effects of p31-43, we used MyD88 KO, IFNαR KO, and Toll-like receptor 4 (TLR4)-deficient (C3H-HeJ) mice. No histological changes were observed in MyD88 KO mice 12 h after administration of p31-43 (Fig. 4*A*). There were no differences in V/C ratio, IEL counts, global histological scores (Fig. 4*B*), or in cell death analysis (Fig. 4*C*) between p31-43- and PBS-treated mice. However, TLR4-deficient C3H-HeJ mice had decreased V/C ratios, increased IELs counts, and increased global histological scores after administration of p31-43 (Fig. 4*D*). The effects of p31-43 were absent in IFNαR KO (Fig. 4*E*).

p31-43 and poly I:C cause mucosal damage via independent mechanisms. Intraluminal administration of poly I:C, a synthetic analog of dsRNA that mimics the innate response to viral infection acting via TLR3 receptor, induces mucosal damage (3). We therefore investigated the effect of intraluminal administration of p31-43 and poly I:C on mucosal damage. On the basis of previous work that determined an optimal time point for the induction of intestinal damage and inflammation with poly I:C and reduced effect of surgery at 72 h (3), we used this time point to evaluate the combined effect of p31-43 and poly I:C. As expected, p31-43-treated mice had reduced V/C ratios compared with control mice at 72 h (Figs. 1*C* and 5*A*), but poly I:C alone or the combination of p31-43 + poly I:C had a more pronounced decrease in V/C ratios (Fig. 5*A*).

p31-43 and poly I:C induce distinct patterns of inflammatory mediators. The analysis of mRNA at different time points after treatment showed distinct patterns of expression for the proinflammatory cytokines IFN-β, IFN-γ, and TNF-α in p31-43-, poly I:C-, or p31-43 + poly I:C-treated mice. Increased expression of IFN-β in the mucosa was found 2 h after treatment with poly I:C, whereas this increase was only noted 4 h after p31-43 + poly I:C treatment. Induction of IFN-β was modest and delayed until 6 h after treatment with p31-43 alone. TNF-α expression was increased by poly I:C or p31-43 + poly I:C but not by p31-43 treatment. Consistent with previous results, p31-43 induced IFN-γ expression, which was not observed in p31-43 + poly I:C-treated or poly I:C-treated mice. Poly I:C is a strong inducer of CXCL10 (8), which was also upregulated by p31-43 + poly I:C treatment, whereas CXCL10 induction by p31-43 was weaker and delayed. A synergistic effect of p31-43 + poly I:C was only observed for CXCL2 and MCP1 (Fig. 5*B*). Altogether, these results suggest that mucosal dam-

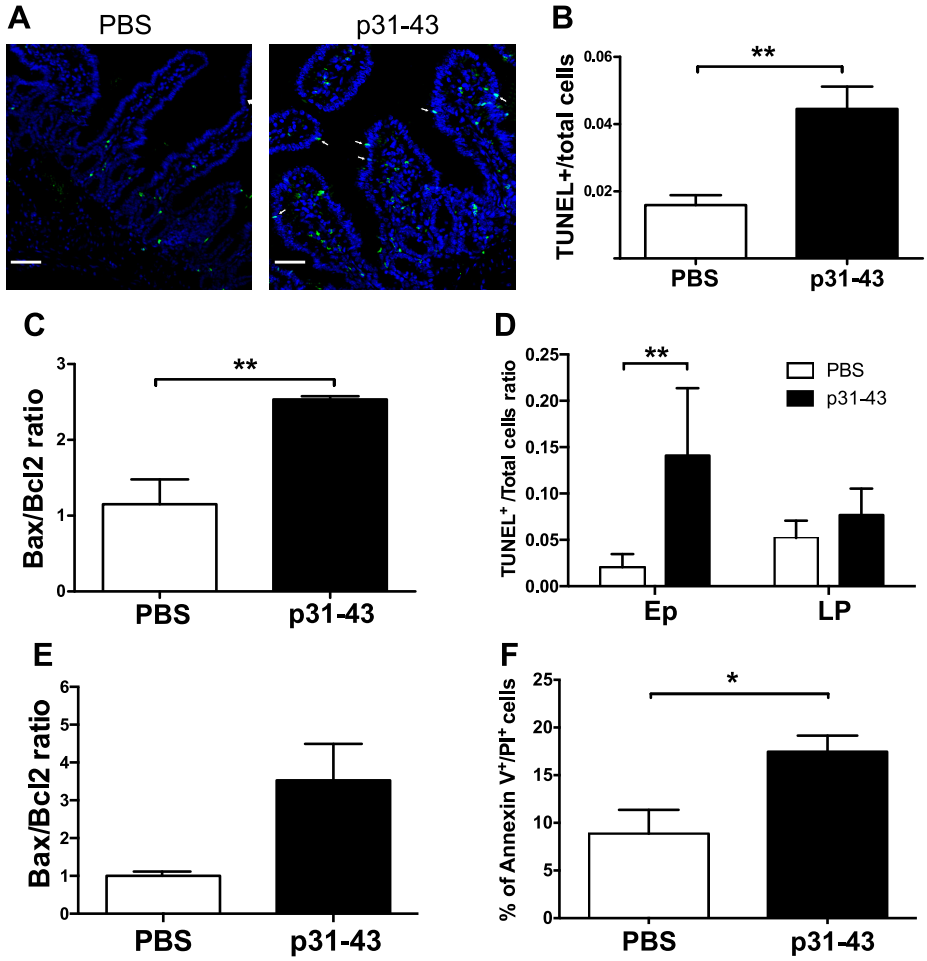

Fig. 3. Intraluminal p31-43 induces cell death in the small intestinal mucosa. Sections of small intestine after 12 h posttreatment with p31-43 or PBS were stained with TUNEL reaction. Sections were analyzed by confocal microscopy. Images were taken from a confocal microscope Olympus FV1000. White arrows point to some TUNEL-positive nuclei in the epithelial layer. Scale bar = 100 μm (*A*). TUNEL-positive/total cells from mucosa were determined using ImageJ software (*B*). The expression of anti- and proapoptotic mediators, Bcl2 and Bax, respectively, was evaluated by quantitative PCR analysis of small intestinal mucosa; results were plotted as Bax/Bcl2 ratio (*C*). TUNEL-positive/total cells from epithelium (Ep) and lamina propria (LP), separately, were determined using ImageJ software (*D*). Epithelial cells were isolated from small intestine 12 h after treatment with p31-43 or PBS, and the expression of Bcl2 and Bax was evaluated by quantitative PCR; results were plotted as Bax/Bcl2 ratio (*E*). Isolated epithelial cells were stained with annexin V and propidium iodide and analyzed by flow cytometry (*F*) ($n = 4$ mice per group, unpaired *t*-test, $^*P < 0.05$, $^{**}P < 0.01$, p31-43-treated mice vs. PBS control).

age caused by p31-43 and poly I:C may employ different pathways, which can interact in a complex fashion.

Poly I:C enhances cell death induced by p31-43. Treatment with p31-43 led to increased cell death in the intestinal mucosa as assessed by TUNEL staining (Fig. 3), and this was further increased in mice given p31-43 + poly I:C together. However, poly I:C alone had no effect on cell death (Fig. 6*A*). Confirming our previous findings, p31-43 alone also induced a proapoptotic pattern of Bax/Bcl2 ratio 12 h after treatment, but this was not seen in mice receiving poly I:C alone or in combination with p31-43 (Fig. 6*B*). On the other hand, treatment with p31-43 + poly I:C induced a marked increase in the number of cleaved-caspase 3-positive cells in lamina propria compared with mice treated with PBS, poly I:C, or p31-43 alone (Fig. 6*C*). As caspase 3 is central to both the intrinsic and extrinsic pathways of apoptosis, these results suggest that p31-43 + poly I:C is a stronger stimulus for cell death than poly I:C or p31-43 alone and that the pathways involved may be different.

DISCUSSION

In this study, we found that intraluminal administration of p31-43 reduced V/C ratio, increased IEL infiltration, and led to higher histological scores in wild-type (C57BL/6) mice. p31-43 caused an inflammatory response in the small intestine, characterized by elevation of IFN-γ expression followed by elevations in IFN-β and CXCL10. p31-43 also induced cell death in epithelial cells. Treatment with p31-43 in mice lacking TLR4 induced similar morphological changes than in wild-type but not in mice lacking the MyD88 molecule. The results indicate a direct proinflammatory effect of p31-43 in vivo that requires the central adaptor of the TLR pathway, MyD88, but is independent of TLR4. Finally, we demonstrated that the mucosal damage induced by p31-43 is type I IFN dependent.

There is controversy on the potential induction of the innate immune response by gliadin peptides. Critiques are based on the lack of specific receptor identification and reports on in vivo effects. p31-43 has been shown to trigger inflammation using cell lines and duodenal biopsies, whereas instillation of p31-49 into the duodenum of treated patients with CD led to reduced V/C ratios and increased IEL counts within 4 h after administration (4, 33). Others have shown that chemokines IP-10 (CXCL10) and MCP-5, which recruit monocytes and T cells, were increased in vitro by p31-43 (34), as well as cell proliferation and proapoptotic activity (4, 6, 12). In this study, we provide evidence for in vivo innate immune stimulation and apoptosis by p31-43. We found that intraluminal p31-43 stimulated a broad spectrum of proinflammatory genes such as *IFNγ*, *CXCL10*, and *IFNβ*, increased the number of Ki-67-positive cells in crypts of C57BL/6 mice, and increased cellular death in lamina propria and in epithelial cells. A high number of TUNEL-positive cells was found in p31-43-treated mice, which was associated with a proapoptotic profile (high Bax/

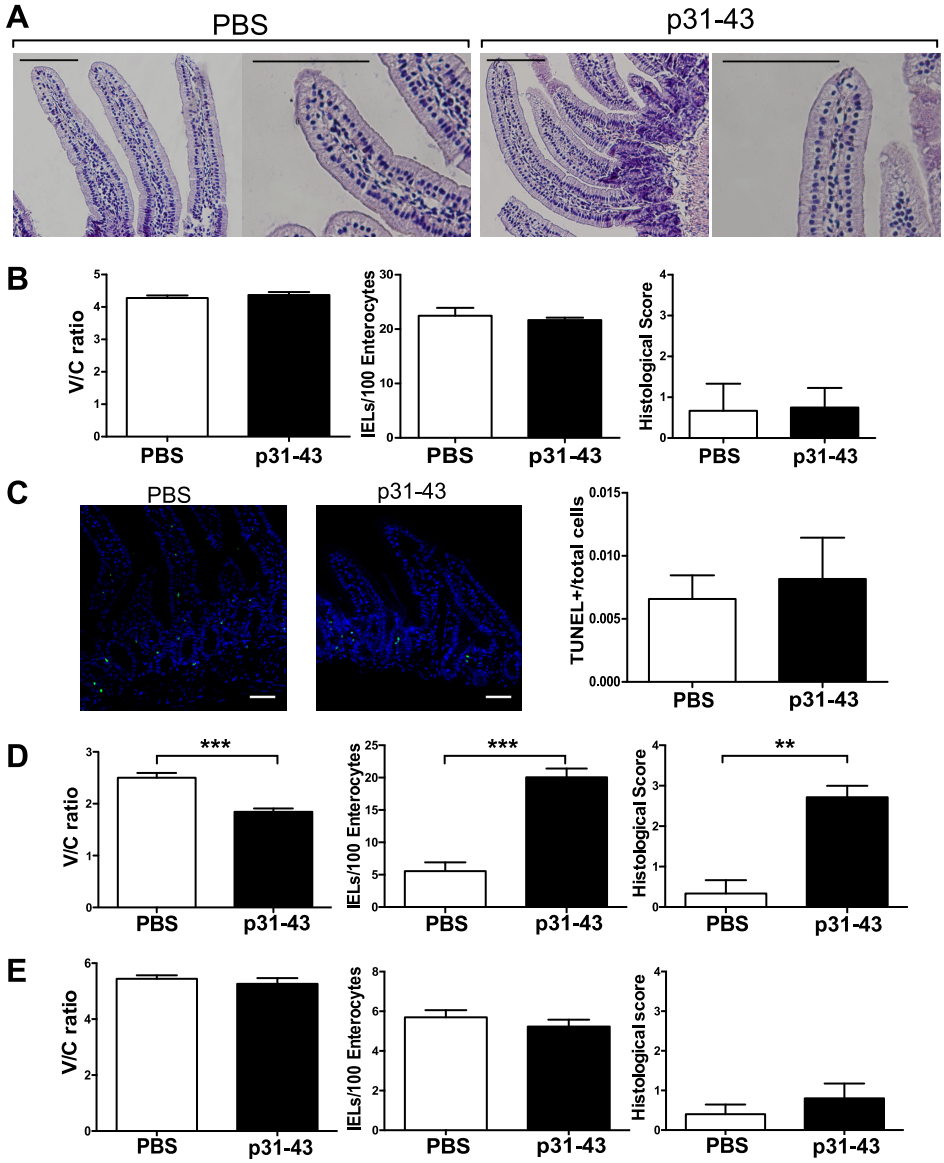

Fig. 4. Changes induced by p31-43 are MyD88 and type I IFN dependent. Representative H and E-stained sections of proximal small intestine of MyD88 mice after 12 and 72 h of intraluminal administration of p31-43 or PBS are shown. Scale bar = 100 μm (*A*). Morphological analysis of small intestine from MyD88 knockout mice treated with p31-43 or PBS included V/C ratio, number of IELs, and histological score after 12 h (*B*). Small intestinal sections after 12 h posttreatment with p31-43 or PBS were stained with TUNEL reaction. Sections were analyzed by confocal microscopy. Images were taken from a confocal microscope Olympus FV1000. Scale bar = 100 μm. TUNEL-positive/total cells from mucosa were determined using ImageJ software (*C*). Morphological analysis of small intestine from C3H/HeJ mice (Toll-like receptor 4-deficient mice) treated with p31-43 or PBS included V/C ratio, number of IELs, and histological score after 12 h (*D*). Morphological analysis of small intestine from IFNαR$^{-/-}$ mice treated with p31-43 or PBS included V/C ratio, number of IELs, and histological score, after 12 h (n = 4 mice per group, unpaired t-test, $^{**}P < 0.01$, $^{***}P < 0.001$).

Bcl2 ratio). Finally, cell death evaluated by qPCR (Bax/Bcl2 ratio), fluorescence microcopy (TUNEL reaction), and flow cytometry (annexin V/propidium iodide) indicated that p31-43 may induce enterocyte death in vivo.

Some previous studies demonstrated that PT-gliadin induced proinflammatory genes in a MyD88-dependent manner but a TLR2- and TLR4-independent manner (34), whereas others showed that gliadin-derived peptides increased inflammatory mediators through TLR4/MyD88/TRIF/MAPK/NFκB and NLRP3 inflammasome pathways (25). Although these findings suggest that innate response via TLR signaling and inflammasome can be elicited by gliadin peptides, p31-43 was not specifically evaluated. Type I IFNs play a critical role in our experimental model, as p31-43 induced the expression of type I IFNs in vivo, and its effects on intestinal pathology were absent in IFNαR KO mice. Type I IFNs have been suggested as early mediators of CD pathogenesis, and MxA, a downstream element of the type I IFN pathway, has been reported to be increased in duodenal biopsies of untreated patients with CD (13). Although it is not known what factors might drive the induction of type I IFNs in patients at risk of CD, viral infection is an obvious potential candidate (15, 31, 32). A role for type I IFNs might also overlap with the proposed involvement of IL-15 in CD (15), as, although these mediators activate different downstream pathways, IL-15 upregulation during experimental virus infection depends on IFNαR signaling (11). Our data suggest that p31-43 and viral infection could act in synergy to induce the innate immune responses such as IL-15 production thought to be critical for the initiation of tissue pathology in CD. To test whether pathways induced by p31-43 and other stimuli synergize to worsen the innate immune response, we employed a poly I:C model (3). We observed distinct proinflammatory patterns in mice with p31-43, poly I:C, or p31-43 + poly I:C treatment. Poly I:C alone increased IFN-β, TNF-α, and CXCL10. p31-43 alone induced IFN-β and CXCL10 at lower levels, and it was the only stimulus that rapidly increased IFN-γ. The combination of p31-43 and poly I:C increased IFN-β, TNF-α, and CXCL10 and was the only stimuli that increased CXCL2 and MCP-1. CXCL10, CXCL2,

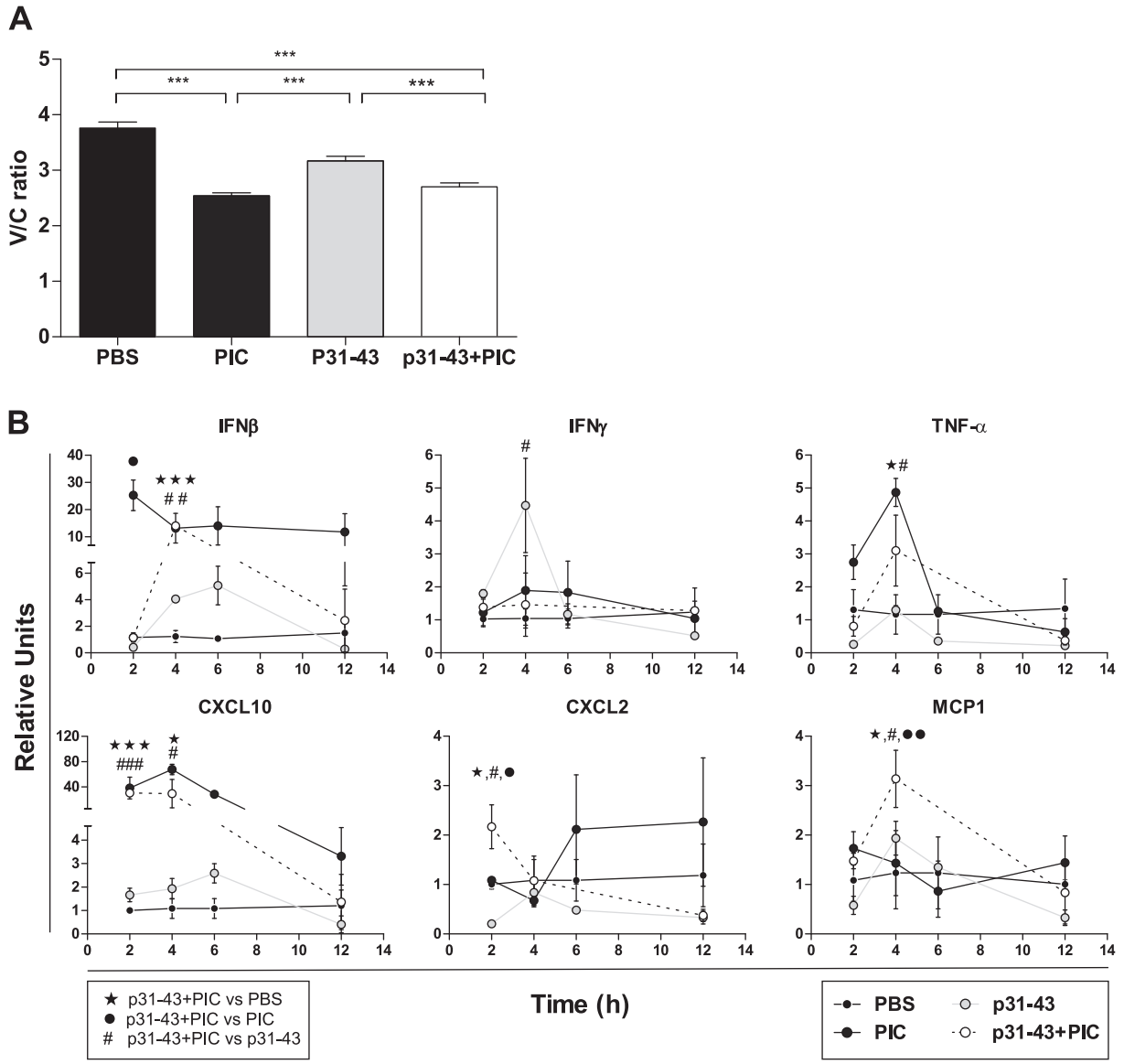

Fig. 5. p31-43 and polyinosinic:polycytidylic acid (poly I:C) cause mucosal damage via independent mechanisms. Morphological analysis of small intestine from C57BL/6 mice after p31-43, poly I:C (PIC), p31-43 + PIC, or PBS treatment is shown. V/C ratio was determined after 72 h ($n = 4$ mice per group, unpaired t-test, $^{*}P < 0.05$, $^{***}P < 0.01$, all treatment vs. PBS control in the same time point) (*A*). Real-time PCR analysis of small intestinal samples from C57BL/6 mice after p31-43, PIC, p31-43 + PIC, or PBS administration is shown. Plots show mRNA expression after 2–12 h of p31-43, PIC, p31-43 + PIC, or PBS treatment. IFN-γ, IFN-β, TNF-α, CXCL10, CXCL2, and MCP1 mRNA expression was assessed. All values were normalized with the housekeeping mRNA expression (HPRT). Results were expressed as fold increase of every treatment vs. the mean of PBS treatment in every time point ($2^{-\Delta\Delta Ct}$ method) ($n = 4$ mice per group, 1-way ANOVA, $\bullet P < 0.05$ and $\bullet\bullet P < 0.01$ p31-43 + poly I:C vs. poly I:C; $^{*}P < 0.05$, $^{***}P < 0.001$ p31-43 + poly I:C vs. PBS; $\#P < 0.05$, $\#\#P < 0.01$, $\#\#\#P < 0.001$ p31-43 + poly I:C vs. p31-43, in the same time point).

and MCP-1 are relevant for the recruitment of T cells, polymorphonuclear cells, and monocytes.

Analysis by TUNEL staining, Bax/Bcl2 ratio, and cleaved caspase-3 suggests that a proapoptotic pathway is involved in the increased cell death observed in p31-43-treated mice. In contrast, poly I:C treatment did not induce a significant increase in any of these parameters, perhaps indicating that the histological damage caused by these stimuli may be driven by different pathways. As well as cell apoptosis, mechanisms such as metalloprotease- and TGF-β-induced fibrosis can all contribute to tissue pathology, and these may be induced differentially by individual triggers. Further support for complexity in the pathogenic processes could come from our finding that, in p31-43 + poly I:C-treated mice, the number of TUNEL-positive cells and of cleaved caspase-3-positive cells was increased, but there was no change in Bax/Bcl2 ratio. Because caspase-3 can be activated by both intrinsic and extrinsic apoptotic pathways, but also can be cleaved by Granzyme B (10), this may explain why in p31-43 + poly I:C-treated mice cleaved caspase-3-positive and TUNEL-positive cells were increased but not the proapoptotic ratio. Together, our results suggest that distinct or partially overlapping pathways of tissue damage may be induced by p31-43 and poly I:C.

The adaptive immune response in CD is necessary for the development of the disease; however, it is now clear that it is insufficient to cause full intestinal pathology (21). Cytotoxic

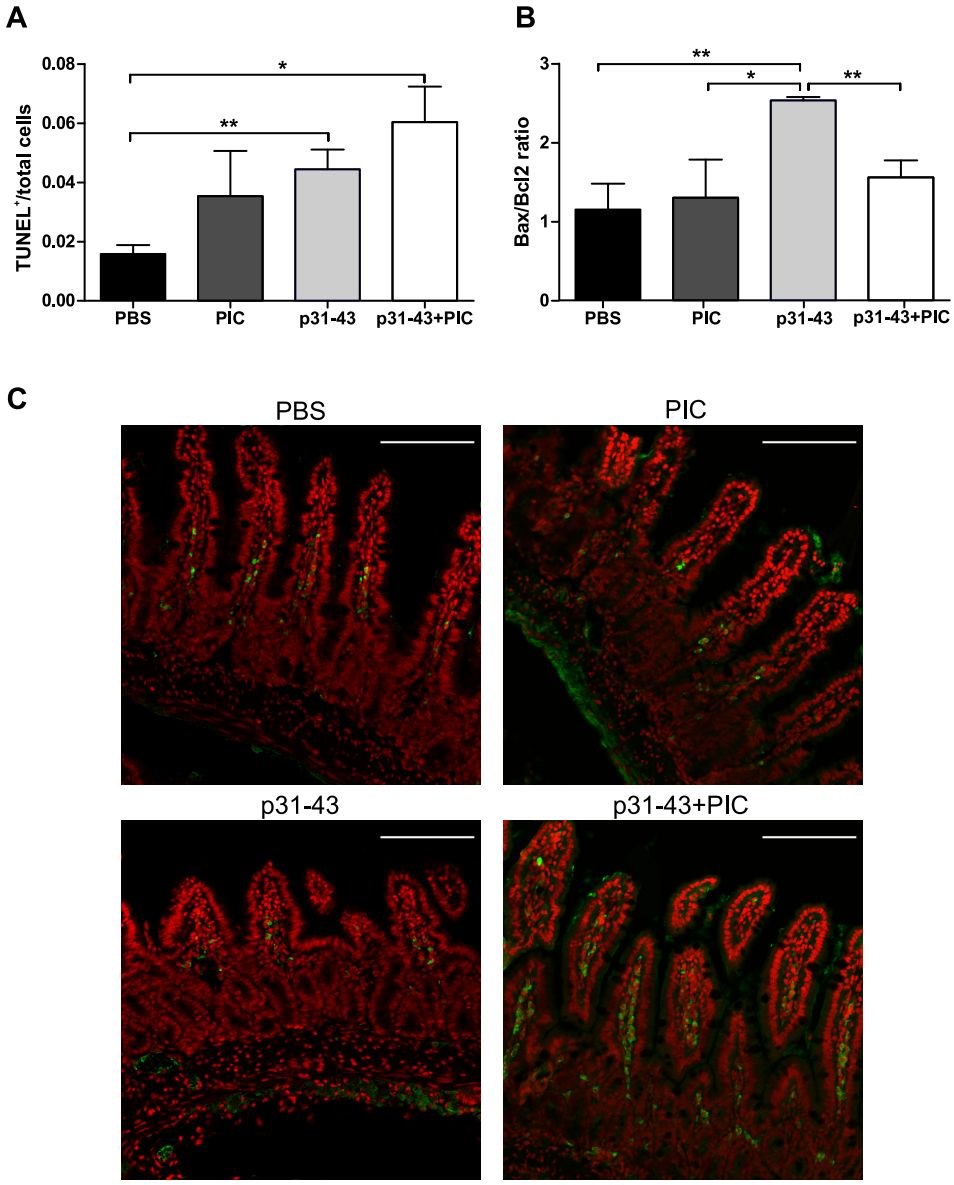

Fig. 6. Poly I:C enhances cell death induced by p31-43. Sections of small intestine after 12 h posttreatment with p31-43 or PBS were stained with TUNEL reaction. Sections were analyzed by confocal microscopy. Images were taken from a confocal microscope Olympus FV1000. Scale bar = 100 μm. TUNEL-positive/total cell ratio was determined using ImageJ software (*A*) ($n = 4$ mice per group, unpaired *t*-test, $*P < 0.05$, $**P < 0.01$, p31-43-treated mice vs. PBS control). The expression of anti- and proapoptotic mediators, Bcl2 and Bax, respectively, was evaluated by quantitative PCR analysis of small intestinal mucosa; results were plotted as Bax/Bcl2 ratio ($n = 4$ mice per group, unpaired *t*-test, $*P < 0.05$, $**P < 0.01$, p31-43-treated mice vs. PBS control) (*B*). Expression of cleaved caspase-3 was assessed by confocal microscopy. Anti-cleaved caspase-3 antibody conjugated to FITC was used. Nuclei were stained with propidium iodide. Images were obtained and analyzed in a TCS SP5 confocal microscope combined with Leica LAS AF software. Scale bar = 100 μm (*C*).

activity of IELs has been considered as a key element for enterocyte damage. Although increased number and activation of IELs are a hallmark of CD, how these cells are induced and activated is still a matter of discussion. Setty et al. (30) have recently suggested that epithelial stress and antigluten adaptive immune responses can be independently induced at early stages of the disease. In accordance with these results, previous reports from our group revealed the presence of epithelial stress in active CD (2). Altogether, the results raise the hypothesis that, by activating innate immunity, peptides such as p31-43 may lead to epithelial stress, a condition that together with the adaptive immune response would facilitate the development of enteropathy in CD. It remains to be determined whether this mechanisms could also have implications for other gluten-related disorders such as non-celiac gluten sensitivity (29). Our work shows that induction of inflammation by nonimmunogenic peptides depends on MyD88, but not TLR4, signaling. In contrast, wheat amylase-trypsin inhibitors have been identified as potent stimulators of an inflammatory reaction through activation of TLR4 signaling on monocytes, macrophages, and dendritic cells (14). Therefore, it is possible that nonimmunogenic gluten peptides and nongluten proteins in wheat induce inflammation through different pathways, facilitating the onset of CD and other intestinal inflammatory diseases.

In summary, in vivo inflammatory changes driven by p31-43 and poly I:C occur through different pathways, as judged by the kinetics of the mucosal damage and histological recovery. Although the receptor for p31-43 has not been identified yet, different cells can produce inflammatory mediators after incubation with this peptide. Because HLA-DQ2 or DQ8 molecules do not present p31-43 and the mucosal changes observed are MyD88 and type I IFN dependent, future work should determine the effect of p31-43 in other genetically modified mouse strains. Signals triggered by gliadin-derived peptides, particularly p31-43, in addition to those elicited by certain infections, may exacerbate inflammation, promoting the development of intestinal pathology in a genetically susceptible individual.

GRANTS

This work was supported by grants to F. Chirdo from CONICET PIP 719 and PICT 2012 1030. E. Verdu is funded by a CIHR grant MOP-142773. R. Araya is a CONICET Scholar. J. McCarville is a Boris Family Scholar.

DISCLOSURES

No conflicts of interest, financial or otherwise, are declared by the authors.

AUTHOR CONTRIBUTIONS

R.E.A., M.F.G.C., P.C., J.L.M., and J.J. performed experiments; R.E.A. and J.J. analyzed data; R.E.A., A.M., E.F.V., and F.C. interpreted results of experiments; R.E.A. prepared figures; R.E.A., E.F.V., and F.C. drafted manuscript; R.E.A., J.L.M., A.M., E.F.V., and F.C. edited and revised manuscript; E.F.V. and F.C. conception and design of research; E.F.V. and F.C. approved final version of manuscript.

REFERENCES

1. **Abadie V, Jabri B.** IL-15: A central regulator of celiac disease immunopathology. *Immunol Rev* 260: 221–234, 2014.
2. **Allegretti YL, Bondar C, Guzman L, Cueto Rua E, Chopita N, Fuertes M, Zwirner NW, Chirdo FG.** Broad MICA/B expression in the small bowel mucosa: a link between cellular stress and celiac disease. *PLoS One* 8: e73658, 2013.
3. **Araya RE, Jury J, Bondar C, Verdu EF, Chirdo FG.** Intraluminal administration of poly i:c causes an enteropathy that is exacerbated by administration of oral dietary antigen. *PLoS One* 9: e99236, 2014.
4. **Barone M, Troncone R, Auricchio S.** Gliadin peptides as triggers of the proliferative and stress/innate immune response of the celiac small intestinal mucosa. *Int J Mol Sci* 15: 20518–20537, 2014.
5. **Barone MV, Gimigliano A, Castoria G, Paolella G, Maurano F, Paparo F, Maglio M, Mineo A, Miele E, Nanayakkara M, Troncone R, Auricchio S.** Growth factor-like activity of gliadin, an alimentary protein: implications for coeliac disease. *Gut* 56: 480–488, 2007.
6. **Barone MV, Zanzi D, Maglio M, Nanayakkara M, Santagata S, Lania G, Miele E, Ribecco MTS, Maurano F, Auricchio R, Gianfrani C, Ferrini S, Troncone R, Auricchio S.** Gliadin-mediated proliferation and innate immune activation in celiac disease are due to alterations in vesicular trafficking. *PLoS One* 6: e17039, 2011.
7. **Biagi F, Luinetti O, Campanella J, Klersy C, Zambelli C, Villanacci V, Lanzini A, Corazza GR.** Intraepithelial lymphocytes in the villous tip: do they indicate potential coeliac disease? *J Clin Pathol* 57: 835–839, 2004.
8. **Bratland E, Hellesen A, Husebye ES.** Induction of CXCL10 chemokine in adrenocortical cells by stimulation through toll-like receptor 3. *Mol Cell Endocrinol* 365: 75–83, 2013.
9. **Bustin SA, Benes V, Garson JA, Hellemans J, Huggett J, Kubista M, Mueller R, Nolan T, Pfaffl MW, Shipley GL, Vandesompele J, Wittwer CT.** The MIQE guidelines: minimum information for publication of quantitative real-time PCR experiments. *Clin Chem* 55: 611–622, 2009.
10. **Clarke P, Tyler KL.** Apoptosis in animal models of virus-induced disease. *Nat Rev Microbiol* 7: 144–155, 2009.
11. **Colpitts SL, Stoklasek TA, Plumlee CR, Obar JJ, Guo C, Lefrançois L.** Cutting edge: the role of IFN-α receptor and MyD88 signaling in induction of IL-15 expression in vivo. *J Immunol* 188: 2483–2487, 2012.
12. **D'Arienzo R, Stefanile R, Maurano F, Luongo D, Bergamo P, Mazzarella G, Troncone R, Auricchio S, David C, Rossi M.** A deregulated immune response to gliadin causes a decreased villus height in DQ8 transgenic mice. *Eur J Immunol* 39: 3552–3561, 2009.
13. **Iacomino G, Marano A, Stillitano I, Aufiero VR, Iaquinto G, Schettino M, Masucci A, Troncone R, Auricchio S, Mazzarella G.** Celiac disease: role of intestinal compartments in the mucosal immune response. *Mol Cell Biochem* 411: 341–349, 2016.
14. **Junker Y, Zeissig S, Kim SJ, Barisani D, Wieser H, Leffler DA, Zevallos V, Libermann TA, Dillon S, Freitag TL, Kelly CP, Schuppan D.** Wheat amylase trypsin inhibitors drive intestinal inflammation via activation of toll-like receptor 4. *J Exp Med* 209: 2395–2408, 2012.
15. **Kim SM, Mayassi T, Jabri B.** Innate immunity: actuating the gears of celiac disease pathogenesis. *Best Pract Res Clin Gastroenterol* 29: 425–435, 2015.
16. **Lammers KM, Khandelwal S, Chaudhry F, Kryszak D, Puppa EL, Casolaro V, Fasano A.** Identification of a novel immunomodulatory gliadin peptide that causes interleukin-8 release in a chemokine receptor CXCR3-dependent manner only in patients with coeliac disease. *Immunology* 132: 432–440, 2011.
17. **Luciani A, Villella VR, Vasaturo A, Giardino I, Pettoello-Mantovani M, Guido S, Cexus ON, Peake N, Londei M, Quaratino S, Maiuri L.** Lysosomal accumulation of gliadin p31-43 peptide induces oxidative stress and tissue transglutaminase-mediated PPARγ downregulation in intestinal epithelial cells and coeliac mucosa. *Gut* 59: 311–319, 2010.
18. **Maiuri L, Ciacci C, Ricciardelli I, Vacca L, Raia V, Auricchio S, Picard J, Osman M, Quaratino S, Londei M.** Association between innate response to gliadin and activation of pathogenic T cells in coeliac disease. *Lancet* 362: 30–37, 2003.
19. **Mamone G, Ferranti P, Rossi M, Roepstorff P, Fierro O, Malorni A, Addeo F.** Identification of a peptide from α-gliadin resistant to digestive enzymes: Implications for celiac disease. *J Chromatogr B Analyt Technol Biomed Life Sci* 855: 236–241, 2007.
20. **Marshall JK, Thabane M, Borgaonkar MR, James C.** Postinfectious irritable bowel syndrome after a food-borne outbreak of acute gastroenteritis attributed to a viral pathogen. *Clin Gastroenterol Hepatol* 5: 457–460, 2007.
21. **Meresse B, Malamut G, Cerf-Bensussan N.** Celiac disease: An immunological jigsaw. *Immunity* 36: 907–919, 2012.
22. **Monteleone G, Pender SL, Alstead E, Hauer AC, Lionetti P, McKenzie C, MacDonald TT.** Role of interferon alpha in promoting T helper cell type 1 responses in the small intestine in coeliac disease. *Gut* 48: 425–429, 2001.
23. **Nanayakkara M, Kosova R, Lania G, Sarno M, Gaito A, Galatola M, Greco L, Cuomo M, Troncone R, Auricchio S, Auricchio R, Barone MV.** A celiac cellular phenotype, with altered LPP sub-cellular distribution, is inducible in controls by the toxic gliadin peptide P31-43. *PLoS One* 8: e79763, 2013.
24. **Nanayakkara M, Lania G, Maglio M, Discepolo V, Sarno M, Gaito A, Troncone R, Auricchio S, Auricchio R, Barone MV.** An undigested gliadin peptide activates innate immunity and proliferative signaling in enterocytes: the role in celiac disease. *Am J Clin Nutr* 98: 1123–1135, 2013.
25. **Palová-Jelínková L, Dáňová K, Drašarová H, Dvořák M, Funda DP, Fundová P, Kotrbová-Kozak A, Černá M, Kamanová J, Martin SF, Freudenberg M, Tučková L.** Pepsin digest of wheat gliadin fraction increases production of IL-1β via TLR4/MyD88/TRIF/MAPK/NF-κB signaling pathway and an NLRP3 inflammasome activation. *PLoS One* 8: e62426, 2013.
26. **Palová-Jelínková L, Rozková D, Pecharová B, Bártová J, Sedivá A, Tlaskalová-Hogenová H, Spísek R, Tucková L.** Gliadin fragments induce phenotypic and functional maturation of human dendritic cells. *J Immunol* 175: 7038–7045, 2005.
27. **Quaedackers JS, Beuk RJ, Bennet L, Charlton A, oude Egbrink MG, Gunn AJ, Heineman E.** An evaluation of methods for grading histologic injury following ischemia/reperfusion of the small bowel. *Transplant Proc* 32: 1307–1310, 2000.
28. **Di Sabatino A, Pickard KM, Gordon JN, Salvati V, Mazzarella G, Beattie RM, Vossenkaemper A, Rovedatti L, Leakey NA, Croft NM, Troncone R, Corazza GR, Stagg AJ, Monteleone G, MacDonald T.** Evidence for the role of interferon-alfa production by dendritic cells in the Th1 response in celiac disease. *Gastroenterology* 133: 1175–1187, 2007.
29. **Sapone A, Lammers KM, Casolaro V, Cammarota M, Giuliano MT, De Rosa M, Stefanile R, Mazzarella G, Tolone C, Russo MI, Esposito P, Ferraraccio F, Cartenì M, Riegler G, de Magistris L, Fasano A.** Divergence of gut permeability and mucosal immune gene expression in two gluten-associated conditions: celiac disease and gluten sensitivity. *BMC Med* 9: 23, 2011.
30. **Setty M, Discepolo V, Abadie V, Kamhawi S, Mayassi T, Kent A, Ciszewski C, Maglio M, Kistner E, Bhagat G, Semrad C, Kupfer SS, Green PH, Guandalini S, Troncone R, Murray JA, Turner JR, Jabri B.** Distinct and synergistic contributions of epithelial stress and adaptive immunity to functions of intraepithelial killer cells and active celiac disease. *Gastroenterology* 149: 681–691; e10, 2015.
31. **Sollid LM, Jabri B.** Triggers and drivers of autoimmunity: lessons from coeliac disease. *Nat Rev Immunol* 13: 294–302, 2013.
32. **Stene LC, Honeyman MC, Hoffenberg EJ, Haas JE, Sokol RJ, Emery L, Taki I, Norris JM, Erlich HA, Eisenbarth GS, Rewers M.** Rotavirus infection frequency and risk of celiac disease autoimmunity in early childhood: A longitudinal study. *Am J Gastroenterol* 101: 2333–2340, 2006.

33. **Sturgess R, Day P, Ellis HJ, Lundin KE, Gjertsen HA, Kontakou M, Ciclitira PJ.** Wheat peptide challenge in coeliac disease. *Lancet* 343: 758–761, 1994.
34. **Thomas KE, Sapone A, Fasano A, Vogel SN.** Gliadin stimulation of murine macrophage inflammatory gene expression and intestinal permeability are MyD88-dependent: role of the innate immune response in Celiac disease. *J Immunol* 176: 2512–2521, 2006.
35. **Verdu EF, Mauro M, Bourgeois J, Armstrong D.** Clinical onset of celiac disease after an episode of Campylobacter jejuni enteritis. *Can J Gastroenterol* 21: 453–455, 2007.